



ParaHydroxyBenzaldehyde Linked via Two Carbon Linker: An Insight in to X-Ray Crystallographic, DFT-Optimization and Hirshfeld Analysis

S. Naveen¹, B. R. Prashantha Kumar², Karthik Kumara³, Santhosh Kumar⁴,
Nanjan M. J.⁵, Lokanath N. K.^{3*}, Abdelkader Zarrouk⁶, Ismail Warad^{7*}

¹Department of Basic Sciences, School of Engg. & Technology, Jain University, Bangalore 562 112, India

²Department of Pharmaceutical Chemistry, JSS College of Pharmacy, Mysuru 570 015, India.

³Department of Studies in Physics, University of Mysore, Manasagangothri, Mysuru 570 006, India

⁴Department of Pharmacy, BITS Pilani, Hyderabad Campus, 500 078, India.

⁵STIFAC CORE, JSS College of Pharmacy, Ootacamund 643 001, India.

⁶LC2AME, Faculty of Science, First Mohammed University, PO Box 717, 60 000 Oujda, Morocco.

⁷Department of Chemistry, Science College, An-Najah National University, P.O. Box 7, Nablus, Palestine.

Received 27 Dec 2017,

Revised 02 Apr 2018,

Accepted 04 Apr 2018

Keywords

- ✓ Para hydroxybenzaldehyde,
- ✓ X-ray diffraction,
- ✓ Hirshfeld surface
- ✓ DFT

lokanath@physics.uni-mysore.ac.in;

warad@najah.edu

Phone: +91 821 2419610;

Fax: +91 821 2419200

Abstract

In the present work, an efficient method to dimerize the parahydroxybenzaldehyde using two carbon linker 1,2-dibromo ethane is reported. The synthetic scheme was optimized to get good yields and the product was purified to get good quality crystals. Further, the molecular structure was confirmed by single crystal X-ray diffraction studies. The 4,4'-(ethane-1,2-diylbis(oxy))dibenzoic acid crystallizes in the monoclinic crystal system, in C2/c space group with unit cell parameters, $a = 16.233(6)$ Å, $b = 11.448(4)$ Å, $c = 7.920(3)$ Å, $\beta = 115.597(13)^\circ$ and $Z = 4$. The crystal structure of the title compound exhibits $\pi \cdots \pi$ and $C-H \cdots \pi$ interactions and contributes to the structural stability. Further, the DFT-structure optimization and Hirshfeld surface analysis were performed for the structure of the desired compound; fingerprint plot reveals the percentage contribution from each individual molecular contact, and it shows that the $H \cdots H$ interactions has the major contribution (30.8%).

1. Introduction

The organic synthesis has become a widely used technique in some of the thrust areas such as drug discovery and drug development processes. Where, structural diversity of compounds is crucial for the small molecule library design intended for high throughput screening against macromolecular targets in lead identification and subsequent lead optimization process [1]. To meet this increasing demand, the efficiency of chemistry is considered to be the most preferred rapid procedure for the creation libraries.

Due to polar functional groups formation, water-soluble di-carboxylic acids organic material, including diphenyl groups, diether part were determined as the most abundant organic aerosol (OA) compounds [2]. The di-carboxylic acid and its derivatives are very important, for example, diamides of di-carboxylic can be used as a new class of material for insecticides against lepidopteron insects [2-6]. The diamides of di-carboxylic were effective in animal models of asthma, inflammation, cancer and infective [4].

In this context, and as a part of our on-going research on such molecules, we have made an attempt to synthesize [3-9] a dimer of para-hydroxyl-benzaldehyde, and its structure was confirmed by X-ray diffraction studies. Further DFT and Hirshfeld analyses were carried out in order to optimized and understand the inter-molecular interactions of the molecule.

2. Experimental

2.1 Materials and method

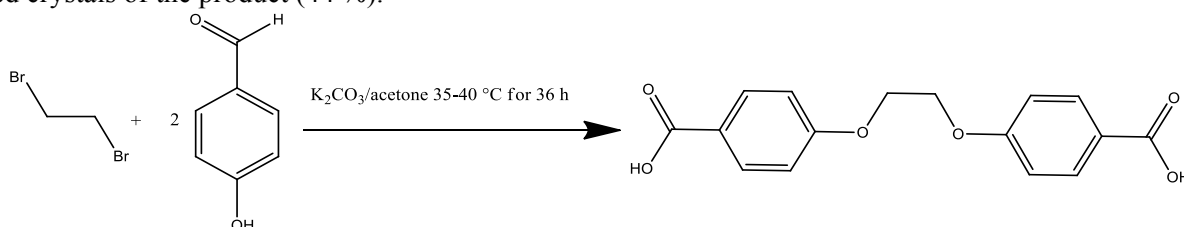
The melting points were measured on a Boetius-Mikroheiztisch the company "VEB" weighing. RapidoRadebeul/VEB NAGEMA. TLC was used for monitoring the reaction mixture which is aluminium foil fluorescent indicator from Merck KGaA (silica gel 60 F254, layer thickness 0.2 mm). R_f -values (run level relative to the solvent front).

2.2 Synthesis of dimer of *p*-hydroxybenzaldehyde

1,2-Dibromo ethane (1 mmol), K_2CO_3 , acetone was stirred at 35-40 °C for 36 h. Two units of *p*-hydroxybenzaldehyde(2 mmol)were inter linked using 1,2-dibromo ethane by taking proportionately more amounts of *p*-hydroxybenzaldehyde using K_2CO_3 as base and dry acetone as solvent to form the product as according to the Scheme 1(44 %).

2.3 Synthetic Procedure and crystallisation

Four equivalents of *p*-hydroxybenzaldehyde were taken in a flat bottomed flask containing four equivalents of finely powdered anhydrous potassium carbonate and sufficient quantity of dry acetone was added to dissolve *p*-hydroxybenzaldehyde. The solution was allowed to stir for 1 h. One equivalent of 1,2-dibromo ethane was added to this. A condenser and a calcium chloride guard tube were then fitted and stirring was continued for about 35 h at 35-40 °C. The reaction was monitored through TLC using 10% ethyl acetate and pet.ether as mobile phase. After the completion of the reaction, the mixture was allowed to cool and the acetone was evaporated. The resulting solid was suspended in sufficient quantity of water and extracted three times with ethyl acetate in a separating funnel. The ethyl acetate layer was washed thrice with 10 % sodium hydroxide solution. The resulting ethyl acetate layer was washed with brine solution and dried over anhydrous sodium sulphate to yield crude solid product. The crude product was separated from the mono substituted product by column chromatography using 5% ethyl acetate in pet ether as mobile phase over silica gel to yield fine needle shaped crystals of the product (44 %).



Scheme 1: Schematic diagram of the 4,4'-(ethane-1,2-diylbis(oxy))dibenzoic acid.

2.4. Single crystal X-Ray diffraction studies

Needle shaped defect free single crystal of approximate dimension 0.33×0.28×0.24 mm was chosen for X-ray diffraction studies. X-ray intensity data for the title compound were collected at temperature 293 K on RigakuXtaLAB Mini diffractometer with X-ray generator operating at 50 kV and 12 mA, using MoK_{α} radiation of wavelength 0.71073 Å. Data were collected with χ fixed at 54° and for different settings of φ (0° and 360°), keeping the scan width of 0.5°, exposure time of 3 s, the sample to detector distance of 50 mm. The compound $C_{16}H_{14}O_6$ crystallized in the monoclinic crystal system, in $C2/c$ space group. The complete intensity data sets were processed using *CRYSTAL CLEAR* [10]. All the frames could be indexed by using a primitive monoclinic lattice. The crystal structure was solved by direct method and refined by full-matrix least squares method on F^2 using *SHELXS* and *SHELXL* programs [11]. The details of the crystal data and structure refinement are as given in Table 1. All the non-hydrogen atoms were refined anisotropically and the hydrogen atoms were positioned geometrically, with C-H = 0.93 – 0.97 Å and refined using a riding model with $U_{iso}(H) = 1.2 U_{eq}(C)$, $U_{iso}(H) = 1.5 U_{eq}(C_{methyl})$. A total of 101 parameters are refined with 1476 unique reflections of 3675 observed reflections. After several cycles of refinement, the final difference Fourier map showed peaks of no chemical significance and the residual is saturated to 0.1252. The geometrical calculations were carried out using the program *PLATON* [12]. The molecular and packing diagrams were generated using the software *MERCURY* [13].

3. Results and discussion

Single crystal X-ray diffraction and DFT-analysis confirms the molecular structure of the title compound $C_{16}H_{14}O_6$. The XRD-ORTEP and DFT-B3LYP/6-311++G(d) DFT-optimized diagrams of the complex are presented in Figure 1. Selected XRD and computed bond lengths and angles are illustrated in Table 2. The list of torsion angles is given in Table 3.

The XRD and DFT reflected the molecule as non-planar. The crystal structure showed the inversion dimers are connected by the c-c bond and are almost perpendicular to each other which is indicated by the torsion angle values of $-73.9(4)^\circ$ for O2-C1-C1-O2. The torsion angle values of $-179.7(4)^\circ$ and $179.9(4)^\circ$ for C4-C5-C6-C9 and C9-C6-C7-C8 confirms that the substituted COOH functional group to the phenyl ring is in the same plane of the ring. The structure exhibits C-H $\cdots\pi$ interactions; C(4)-H(4) \cdots Cg1 (Cg1 is the centroid of the ring C3/C4/C5/C6/C7/C8), with a C—Cg distance of 3.7491 Å, H \cdots Cg distance of 2.92 Å, C—H \cdots Cg angle of 150°, and with a symmetry code $X, -Y, -1/2 + Z$. The molecular structure is also involving $\pi\cdots\pi$ stacking

interactions; $Cg(1)–Cg(1)$ with $Cg–Cg$ distance of 3.7197 Å and symmetry code 1/2-X,1/2-Y,-Z . These interactions contribute to the structural stability. The packing of the molecules viewed along b and c -axis are as shown in Figure 2.

Table 1: Crystal data and structure refinement details

Parameter	Value
CCDC No.	1811804
Empirical formula	$C_{14}H_{14}O_6$
Formula weight	302.27
Temperature	293 K
Wavelength	0.71073 Å
Crystal system, space group	Monoclinic, $C2/c$
Unit cell dimensions	$a = 16.233(6)$ Å. $b = 11.448(4)$ Å
Volume	$1327.4(9)$ Å ³
Z	4
Density (calculated)	1.513 Mg m ⁻³
Absorption coefficient	0.117 mm ⁻¹
$F(000)$	632
Crystal size	$0.33 \times 0.28 \times 0.24$ mm
θ range for data collection	3.13° to 27.48°
Index ranges	$-9 < h < 21$, $-13 < k < 14$, $-10 < l < 10$
Reflections collected	3675
Independent reflections	1471 [R int = 0.0889]
Absorption correction	multi-scan
Refinement method	Full matrix least-squares on F^2
Data / restraints / parameters	1476 / 0 / 101
Goodness-of-fit on F^2	1.091
Largest diff. peak and hole	0.477 and -0.538 e Å ⁻³

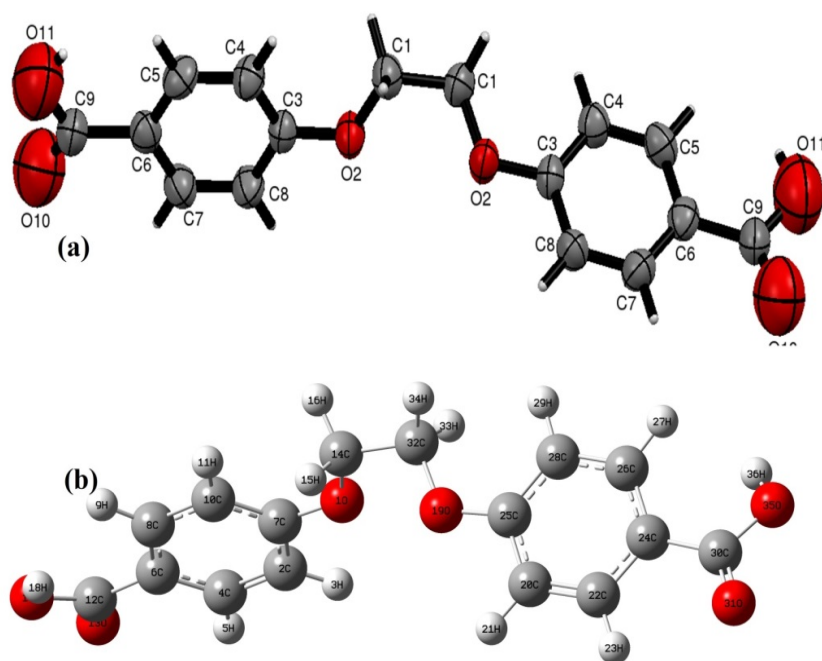


Figure 1. ORTEP of the molecule with thermal ellipsoids drawn at 50% probability.

Table 2: Selected DFT and XRD angles and bond lengths.

Bond no.	Bond type		DFT [Å]	XRD [Å]	Angle no.	Angle type			XRD (°)	DFT (°)
1	O1	C7	1.3582	1.367	1	C3	O2	C1	117.7	119.22
2	O1	C14	1.4227	1.423	4	C7	C8	C3	119.9	120.18
4	C2	C4	1.381	1.372	6	C8	C7	C6	120.8	120.91
5	C2	C7	1.403	1.389	8	C7	C6	C5	119.1	118.44
7	C4	C6	1.4037	1.388	9	C7	C6	C9	119.9	117.92
8	C6	C8	1.3963	1.399	10	C5	C6	C9	121	123.59
9	C6	C12	1.4949	1.481	11	O2	C3	C8	115.5	115.7
10	C7	C10	1.398	1.384	12	O2	C3	C4	124.2	124.64
12	C8	C10	1.3934	1.387	13	C8	C3	C4	120.3	119.65
14	C12	O13	1.201	1.25	15	C6	C5	C4	120.2	121.3
15	C12	O17	1.363	1.3	17	C3	C4	C5	119.7	119.5
18	C14	C32	1.5104	1.52	20	C6	C9	O10	123.1	123.6
20	O19	C25	1.3582	1.367	21	C6	C9	O11	121.7	116.54
21	O19	C32	1.4227	1.423	22	O10	C9	O11	113.8	119.86
23	C20	C22	1.381	1.372	25	O2	C1	C1	107.6	107.91
24	C20	C25	1.403	1.389	30	C3	O2	C1	117.7	119.22
26	C22	C24	1.4037	1.388	33	C7	C8	C3	119.9	120.18
27	C24	C26	1.3962	1.399	35	C8	C7	C6	120.8	120.91
28	C24	C30	1.4949	1.481	37	C7	C6	C5	119.1	118.44
29	C25	C28	1.398	1.384	38	C7	C6	C9	119.9	117.92
31	C26	C28	1.3934	1.387	39	C5	C6	C9	121	123.59
33	C30	O31	1.201	1.25	40	O2	C3	C8	115.5	115.7
34	C30	O35	1.363	1.3	41	O2	C3	C4	124.2	124.64
					42	C8	C3	C4	120.3	119.65
					44	C6	C5	C4	120.2	121.3
					46	C3	C4	C5	119.7	119.5
					49	C6	C9	O10	123.1	123.6
					50	C6	C9	O11	121.7	116.54
					51	O10	C9	O11	113.8	119.86
					52	C1	C1	O2	107.6	107.91

Table 3: XRD torsion angles (°).

Atoms	Angle	Atoms	Angle
C3-O2-C1-C1	-172.1(3)	C4-C5-C6-C7	-0.1(7)
C1-O2-C3-C4	-3.7(5)	C4-C5-C6-C9	-179.7(4)
C1-O2-C3-C8	176.5(4)	C5-C6-C7-C8	0.3(7)
O2-C1-C1-O2	-73.9(4)	C9-C6-C7-C8	179.9(4)
O2-C3-C4-C5	178.2(4)	C5-C6-C9-O10	166.3(6)
C8-C3-C4-C5	-2.0(6)	C5-C6-C9-O11	0.7(8)
O2-C3-C8-C7	-177.9(4)	C7-C6-C9-O10	-13.3(8)
C4-C3-C8-C7	2.2(6)	C7-C6-C9-O11	-178.9(6)
C3-C4-C5-C6	0.9(7)	C6-C7-C8-C3	-1.4(7)

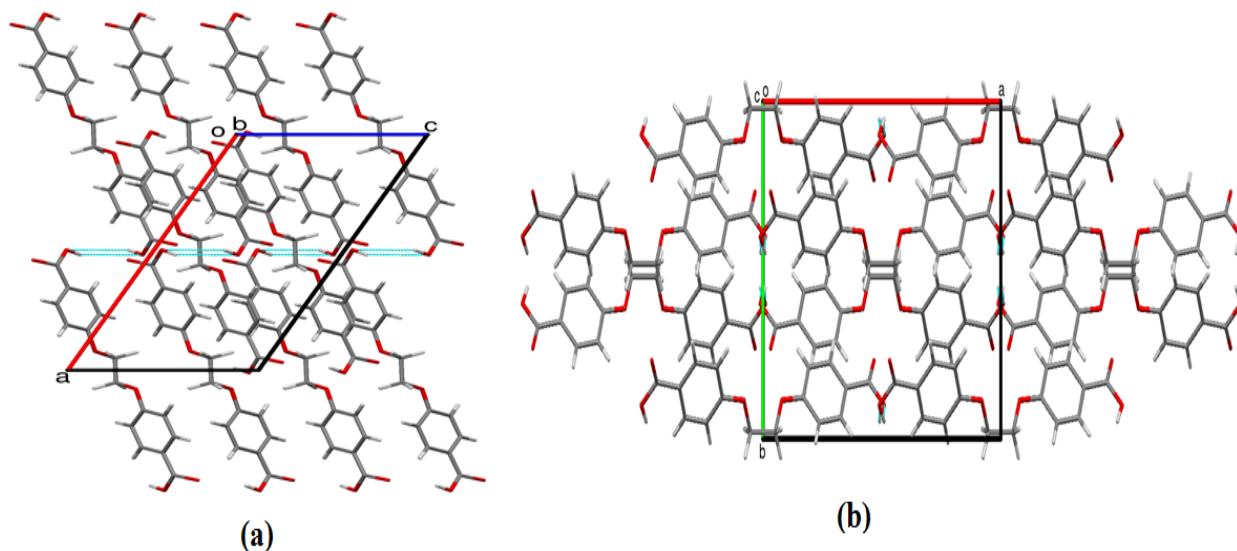


Figure 2. The packing of the molecules when viewed down the *b*-axis (a) and *c*-axis (b). The dotted lines indicating the molecular interactions

Good harmony between XRD and DFT data like angles and bond lengths were recorded as seen in Figure. Most of the experimental and calculated bonds are close in their values (Figure 3a). Very good matching between XRD and DFT angles are reported with $R^2 = 0.92$, as illustrated in Figure 3b.

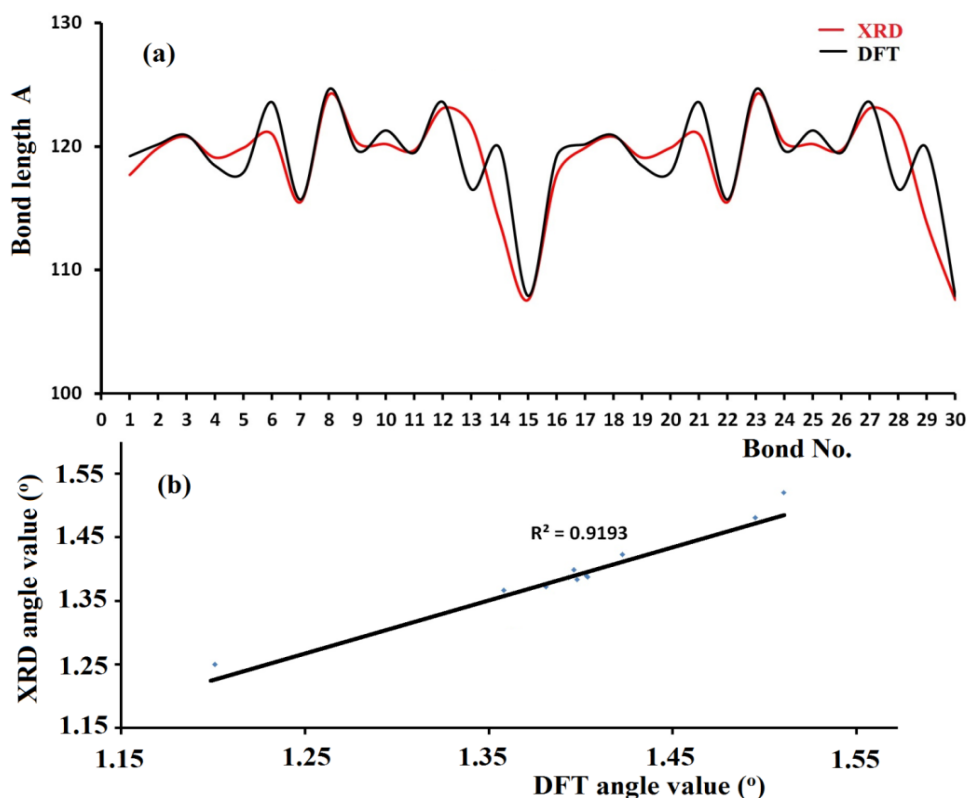


Figure 3. (a) XRD *vis.* DFT-bonds lengths relations and (b) XRD-angles *vis.* DFT-angles graphical correlation.

Hirshfeld surface studies

Hirshfeld surface analysis (HSA) is a computational tool, which helps to understand intermolecular forces apart from their graphical visualization. Analysis and calculations of the HSA were carried out and fingerprints were plotted using CrystalExplorer 3.0 program [10]. The d_{norm} plots were mapped with color scale in between -1.105 au (blue) to 0.901 au (red) respectively. The expanded 2D fingerprint plots [11, 12] were displayed in the range of 0.6 – 2.8 Å with the d_e and d_i distance scales displayed on the graph axes. d_i is the closest

internal distance from a given point on the Hirshfeld surface and d_e is the closest external contacts [13-16]. The fingerprint plots reveal the percentage contribution of intermolecular contacts to the surface which can be represented in terms of color codes. The $H\cdots H$ (30.8%) contacts has maximum and $C\cdots O$ (4.7%) has minimum contributions. Similarly the $O\cdots H$ (30.5%), $C\cdots H$ (19.9%), $C\cdots C$ (7.2%) and $O\cdots O$ (6.8%) contacts contribute to the total area of the surface as shown in Figure 4. These contacts are highlighted on the molecular surface using conventional mapping of d_{norm} , shape index and curvedness as shown in the Figure 5. The regions with red and blue color represent the shorter and longer inter contacts [16-24].

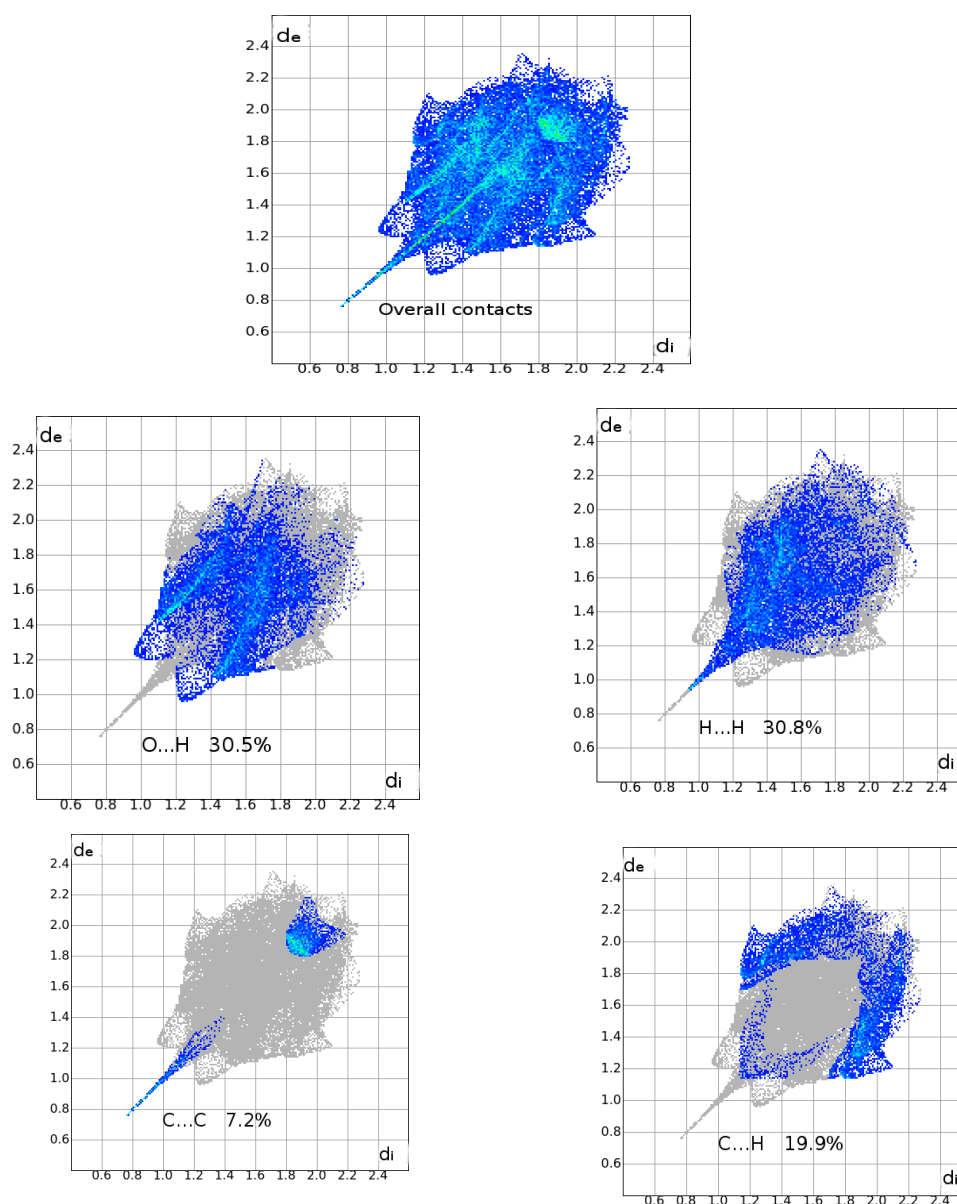


Figure 4. Fingerprint plots and corresponding surface area of the title compound.

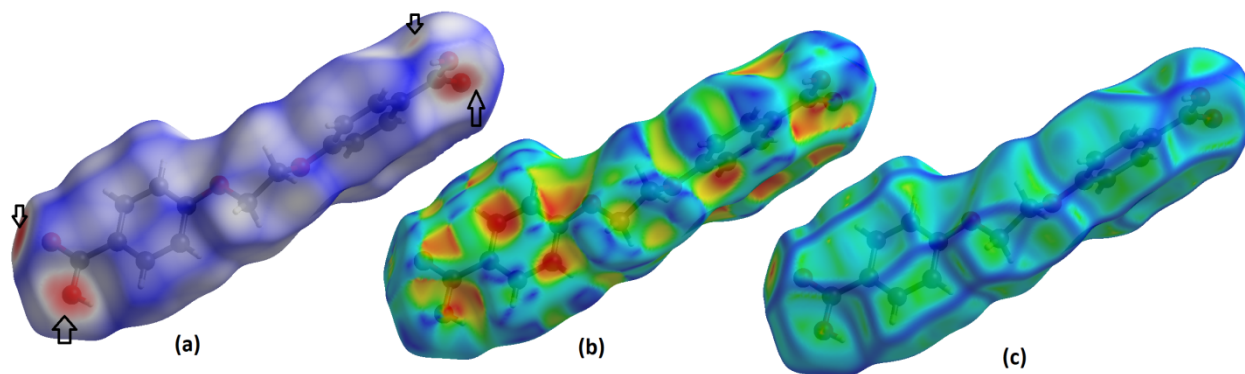


Figure 5. d_{norm} , shape index and curvedness mapped on Hirshfeld surface visualizing the molecular contacts.

Conclusions

The 4,4'-(ethane-1,2-diylbis(oxy))dibenzoic acid has been synthesized and the single crystals were grown by the slow evaporation method using ethyl acetate in ether as a solvent. The molecular structure of the compound was confirmed by the single crystal X-ray diffraction studies, which revealed that the compound crystallized in the monoclinic crystal system, in $C2/c$ space group. The crystal and molecular structure of the compound is stabilized by the $\pi\cdots\pi$ and $C-H\cdots\pi$ interactions. The DFT-optimization structure was found to be consistent with the XRD solved one. The analysis of the Hirshfeld surface; fingerprint plots of the molecule confirms the presence of these interactions, the major share for the surface being from $H\cdots H$ (30.8%).

Acknowledgements: The authors are grateful to the National Single Crystal Diffractometer Facility, Department of Studies in Physics, University of Mysore, Manasagangotri, Mysuru for providing X-ray intensity data. The authors are also thankful to DST-FIST for providing financial support under research grant scheme Project No. **SR/FST/ETT-378/2014**.

References

1. P. Kumar, P. Basu, L. Adhikary, M.J. Nanjan, *Synth. Comm.* 42(2012) 3089-3096.
2. Feng, Qi, Liu, Zhi-Li, Xiong, Li-Xia, Wang, Ming-Zhong, Li, Yong-Qiang, Li, Zheng-Ming, *J. Agric. Food Chem.* 58 (2010) 12327-12336.
3. F. Mei-Li, L. Yu-Feng, Z. Hong-Jun, Z. Liang, X. Bin-Bin, N. Jue-Ping, *J. Agric. Food Chem.* 58, (2010) 1099–11006.
4. P. Gale, S. Garcí-Garrido, J. Garric, *Chem. Soc. Rev.* 37 (2008) 151.
5. G. Kumares, S. Avik Ranjan, P. Amarendra, *Tetrahedron Lett.* 50 (2009) 6557–6561.
6. P. Kumar, S. Kumar, M.J. Nanjan, *Med. Chem. Res.* 21 (2012) 2689–2701.
7. S. Naveen, S. Pavithra, M. Abdoh, A. Kumar, I. Warad, N.K. Lokanath, *Acta Cryst.* E71 (2015) 763-765.
8. I. Warad, F. Al-Rimawi, A. Barakat, S. Affouneh, S. Naveen, N.K. Lokanath, I. Abu-Reidah, *Chem. Central J.* 10:38 (2016) 1-11.
9. S. Naveen, D. Achutha, A. Kumar, N. K. Lokanath, *Chem. Data Coll.*, 3 (2016) 1-7.
10. Rigaku. *CRYSTAL CLEAR*. 2011, Rigaku Corporation, Tokyo, Japan.
11. G. M. Sheldrick, *Acta. Crystallogr. Sec. C: Str. Chem.*, 71 (2015) 3-8.
12. A. L. Spek, *Acta. Crystallogr. Sec. D: Bio. Crystallogr.*, 65 (2009) 148-55.
13. C. Macrae, P. Edgington, P. McCabe, E. Pidcock, G. Shields, R. Taylor, M. Towler, J. Streek, *J. Appl. Cryst.*, 39 (2006) 453-457.
14. S. Wolff S, D. Greenwood, J. McKinnon, M. Turner, D. Jayatilaka, Spackman M. A., *Crystal Explorer* (2012).
15. S. K. Seth, *Cryst. Eng. Comm.*, 15 (2013) 1772–1781.
16. S. K. Seth, *J. Mol. Str.*, 1064 (2014) 70-75.
17. D. Jayatilaka, D. Grimwood, A. Lee, A. Lemay, A. Russell, TONTO, The University of Western Australia, Nedlands (2005).
18. D. K. Achutha, K. Kumara, S. Naveen, N.K. Lokanath, A.K. Kariyappa, *Chem. Data Coll.*, 9 (2017) 89-97.
19. M. A. Spackman, D. Jayatilaka, *Cryst. Eng. Comm.*, 11 (2009) 19–32.
20. A. Janim, M. Al-Nuri, A. BaniOdeh, S. A. Barghouthi, M. Ayes, A. Al Ali, S. Amereih, I. Warad, *J. Mater. Environ. Sci.* 7 (2016) 3447-3453.
21. A. Barakat, S. M. Soliman, H. A. Ghabbour, M. Ali, A. M. Al-Majid, A. Zarrouk, I. Warad, *J. Mol. Struct.* 1137 (2017) 354–361.
22. A. Barakat, A. M. Al-Majid, M. Sh. Islam, I. Warad, V. H. Masand, S. Yousuf, M. I. Choudhary, *Res. Chem. Intermed.* 42 (2016) 4041–4053.
23. M. Al-Noaimi, A. Nafad, I. Warad, R. Alshwafy, A. Husein, W. H. Talib, T. B. Hadda, *Spectrochim. Acta Mol. Biomol. Spectrosc.* 122 (2014) 273–282.
24. M. Al-Noaimi, M. Choudhar, F. Awwadi, W. Talib, T. B. Hadda, S. Yousuf, A. Sawafta, I. Warad, *Spectrochim. Acta Mol. Biomol. Spectrosc.* 127 (2015) 225-232.

(2018) ; <http://www.jmaterenvironsci.com>